We N116 05

Diffraction Imaging of the Zhao Dong Field, Bohai Bay, China

M.A. Pelissier (Roc Oil (Bohai) Company), T.J. Moser* (Moser Geophysical Services), L. Jing (PetroChina), P. de Groot (dGB Earth Sciences), A. Sirazhiev (dGB Earth Sciences), I. Sturzu (Z-Terra Inc.) & A.M. Popovici (Z-Terra Inc.)

SUMMARY

We provide an overview of integrated pre-stack depth migration and diffraction imaging for the Zhao Dong field, Bohai Bay, China. This field is highly compartmentalized by a complex faulting. The objective of the diffraction imaging is to better define these faults. Tools to facilitate interpretation include displays with pre-stack depth migration and diffraction images overlain in different colour scales, the combination of pre-stack depth migration and diffraction images into a single volume and a diffraction image obtained with a spatially varying taper calibrated to local reflectivity.

Introduction

This paper provides an overview of integrated pre-stack depth migration (PSDM) and diffraction imaging seismic re-processing for the Zhao Dong field, located in Bohai Bay, off the north-eastern coast of China. This field is highly compartmentalized by a complex faulting. The objective of the diffraction imaging is to better define these faults. For the deeper reservoirs, there is also the objective of identifying fine scale faulting that may be associated with sub-seismic fracturing. Tools to facilitate interpretation include displays with PSDM and diffraction images overlain in different colour scales, the combination of PSDM and diffraction images into a single volume and a diffraction image obtained with a spatially varying taper calibrated to local reflectivity.

Overview of the Zhao Dong field and the role of faulting

The Zhao Dong field is located in Bohai Bay, off the northeastern coast of China. The field is a faulted anticline. The faults serve to compartmentalize the field into more than 80 productive pools across a large number of discrete reservoirs in the Cenozoic and Mesozoic. The pools are typically produced by horizontal wells, with pressure support from high angle injectors. The fault interpretation plays a critical role in the well planning for existing pools and in identification of prospective new pools . The Neogene reservoir consists largely of fluvial deposits, ranging from unconsolidated meandering channels to consolidated, amalgamated sands. The Paleogene reservoirs include fluvial, lacustrine and deltaic environments. The Cretaceous and Jurassic reservoirs include fluvial and lacustrine environments. Whereas the Neogene reservoirs are characterized by excellent porosities, the deeper reservoirs have generally poor matrix porosities, with local areas of fracture porosity. The identification of small scale faults possibly also associated with sub-seismic fractures is also an objective of the diffraction imaging. With reservoirs depths mostly in the 1000-2000m range and a simple overburden and velocity field, the Zhao Dong field is a natural candidate for diffraction imaging.

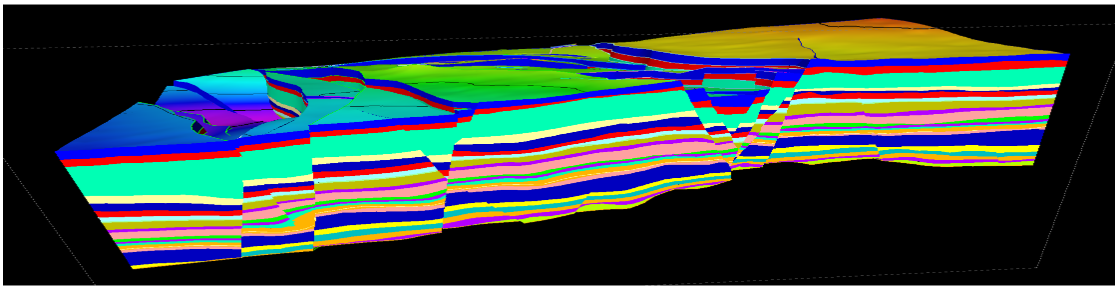

***Figure 1** Zhao Dong field geomodel.*

Diffraction and specularity concepts

Diffractions are characterized as the seismic response from subsurface discontinuities that does not satisfy Snell's law for specular reflection, or for which the angle of incidence differs from the angle of reflection. On the one hand this characterization identifies diffractions as carriers of information from small structural elements which are important for interpretation, such as faults (Khaidukov et al., 2004). On the other hand, the deviation from Snell's law can be used in migration to image diffractions separately from the main wave field and thus obtain a diffraction image. In Sturzu et al. (2013), the term *specularity* is defined as the agreement with Snell's law and quantified as the cosine of the angle between the local reflector normal and the bisector of ray vectors to source and receiver. This quantity is unity for pure specular reflections and less than one for non-specular diffractions. Sorting the output of pre-stack migration with respect to specularity, in so-called *specularity gathers*, enables the design of tapers of specular reflection energy after migration and thus the efficient construction of an optimal diffraction image. Design parameters of the tapers include acquisition geometry and local Fresnel zone width. For details and references, see Sturzu et al. (2013). For an application of diffraction imaging on unconventional reservoirs, see Sturzu et al. (2014).

Pre-stack Depth Migration and Diffraction Imaging Workflow

The diffraction imaging over the Zhao Dong field was carried out in depth domain (Moser and Howard, 2008). The key ingredient in diffraction imaging in depth is an optimal migration velocity obtained from preceding standard pre-stack depth migration. In this concept, the focusing and quality of the diffraction image depends fully on the focusing and quality of the standard migration. First the common workflow for pre-stack depth migration of the full wave field is completed. For the Zhao Dong field this involved the merge of several surveys, a diffraction-friendly preprocessing, a number of tomographic updates to obtain an optimal migration velocity model and the final migration itself. The next step is to extract a reflector dip field from the migrated image, that is, the reflector unit normal at any point in the image. The third step is another run of the pre-stack migration, but with a modified migration kernel, in the sense that the migration output is sorted with respect to specularity and exported as specularity gathers. Based on the specularity gathers, an optimal taper was designed to produce the diffraction image.

Simultaneous interpretation of reflections and diffractions

In interpreting images from reflection and diffraction data, we can exploit the fact that the two wavefields generally complement each other. This is illustrated in Figure 2. Here we can observe that the areas of low and chaotic reflectors on the PSDM in many cases are geologically meaningful, in that they correspond to strong events on the diffraction image. (In Figures 2, 3, 4 and 6, the vertical and horizontal bars denote a length scale of 1000 m).

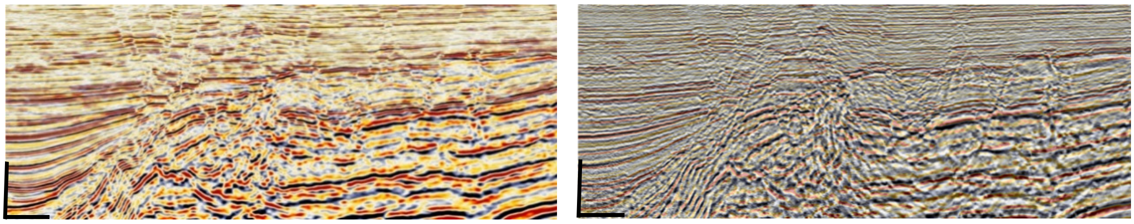

Figure 2 *a) PSDM, b) PSDM with semi-transparent diffraction image overlay.*

The diffraction imaging brings out a very significant additional level of detail and resolution in the faulting of both large and small scale faults. Large scale faults can more readily be extended from the near surface to the basement. In many areas we observe closely spaced faults not detected or resolved on the coherence attribute. The faulting areas of low reflectivity become very apparent on the diffraction image. A number of low amplitude areas in the Mesozoic is associated with areas of dense faulting. This is sometimes the result of the convergence on intersecting sets of faults.

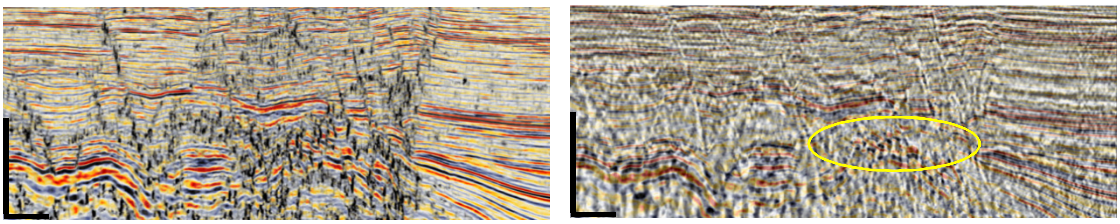

Figure 3 *a) PSDM with coherence overlay b) PSDM with diffraction image overlay.*

Interpreters often use attributes such as similarity or coherence to help detect discontinuities on seismic reflection images. It is useful to compare and contrast this type of attribute with the information contained in the diffraction image. Areas with poor reflection coherence are associated with the larger scale discontinuities. Although these are detectable by coherence, the coherence attribute does not have the spatial resolving power of the diffraction image. In areas of high coherence, diffractions are associated with fine scale discontinuities. The fact that the reflectors here appear to be continuous means that coherence completely fails in these areas; fine scale discontinuities are not even detectable by coherence. This is illustrated in Figure 3. Here the diffraction image serves to highlight densely faulted areas of Mesozoic reservoir.

A second example comparison of coherence to the diffraction image is shown in Figure 4. Here we can observe that an antithetic fault can be interpreted on the diffraction image, but is not detected by coherence. This is likely to be a fault with a very small throw, but nevertheless important to be recognized in well planning.

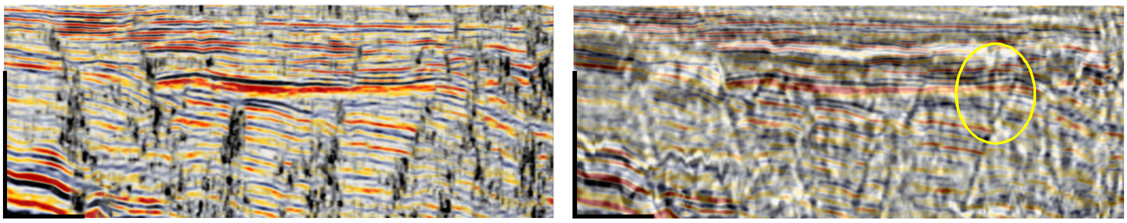

Figure 4 *a) PSDM with coherence overlay b) PSDM with diffraction image overlay.*

In trying to develop integrated interpretation workflows for Zhao Dong, and for PSDM and diffraction imaging in general, we have investigated the possibility of conditioning the poor coherent energy around faults. This is an adaptation of approaches such as the van Gogh filter (Fehmers and Höckers, 2003). In areas of poor reflection coherence in the vicinity of faults, we generally have strong diffraction energy due to the bed terminations against the faults. Figure 5a shows the histogram for the coherence attribute over the Zhao Dong field for a subset containing most of the producing reservoirs. The low coherence outliers occupy only a very small fraction of the data volume. Below a certain coherence level, we can gradually replace the reflection signal by the diffraction signal. The blending function concept is shown in Figure 5b. In areas of high reflectivity, the full weight is given to the PSDM. This range includes the reservoirs, and we can apply quantities methods such as seismic inversion within this range. Around significant faults, we provide an increasing weight to the diffraction image.

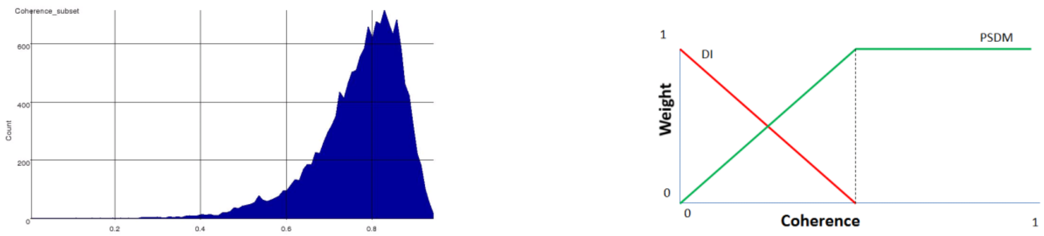

Figure 5 *a) Coherence attribute histogram for Zhao Dong, 500-1200 m interval b) blending function.*

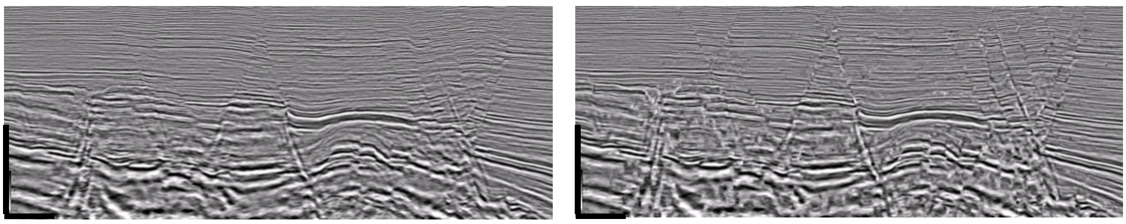

Figure 6 *a) PSDM b) PSDM and diffraction image blended according to coherence.*

An example of the composite PSDM and diffraction imaging is shown in Figure 6. This method has the advantage of providing a single volume for basic interpretation. The details of the major faults are much better defined that in the PSDM alone. Although coherence is used in the preparation, the level of resolution is higher than that provided by coherence. In using this type of composite volume, we need to keep in mind that none of diffraction image of faults from the high reflectivity, high coherence part of the volume are included. In other words, we have not included the part of the diffractivity associated with fine scale discontinuities, and have in fact excluded most of the diffractivity in the seismic volume.

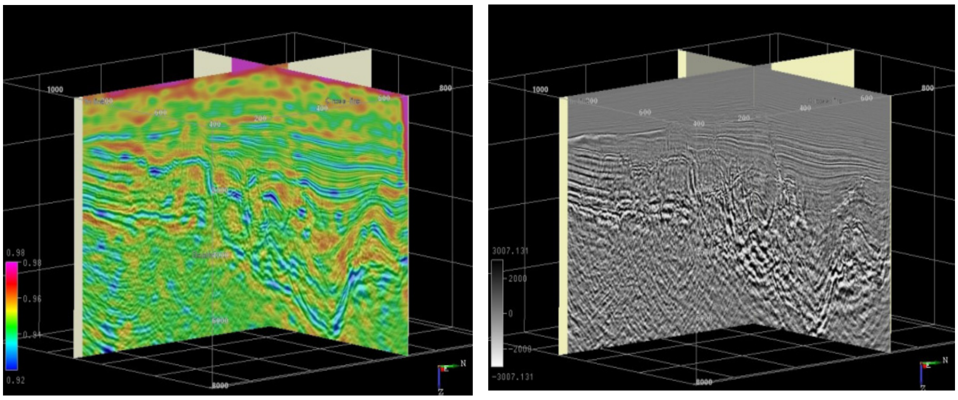

***Figure** 7 a) Variable specularity taper b) Diffraction image obtained with variable specularity taper .*

A robust alternative to a blending of the reflection and diffraction images is to use a spatially varying specularity taper in the diffraction imaging. In this approach we design the specularity taper in relation to the local Fresnel zone width so that strong coherent reflection energy is suppressed more progressively than less coherent energy. This enables us to obtain a diffraction image which is optimally and faithfully calibrated against local reflectivity. This is illustrated by the specularity taper in Figure 7a (blue denotes areas of strong reflectivity and strong taper, red denotes a weak taper) and corresponding diffraction image in Figure 7b.

Conclusions

The combined use of PSDM and diffraction imaging has substantially improved the level of fault definition of the Zhao Dong field. Many aspects of the graben structure have been improved. Small scale faulting is evident in the Mesozoic reservoirs. We expect that the integrated use of PSDM and diffraction imaging will generate a step change in high-resolution and high-fidelity interpretation, in combination with diffraction modeling for validation and quality control, along the lines promoted in Grasmueck et al. (2015).

Acknowledgements

We would like to thank Roc Oil (Bohai) and PetroChina for permission to show the Bohai Bay seismic data.

References

Fehmers, G. C. and Höckers, C. [2003] Fast structural interpretation with structure-oriented filtering, *Geophysics*, **68**, 1286–1293.

Grasmueck, M., Moser, T.J., Pelissier, M.A., Pajchel, J. and Pomar, K., [2015] Diffraction signatures of fracture intersections, *Interpretation*, **3**, 1-14.

Khaidukov, V., Landa, E. and Moser, T.J. [2004] Diffraction imaging by focusing-defocusing: An outlook on seismic superresolution, *Geophysics*, **69**, 1478-1490.

Moser, T.J. and Howard, C.B. [2008] Diffraction imaging in depth, *Geophysical Prospecting*, **56**, 627-641.

Sturzu, I., Popovici, A.M., Tanushev, N., Musat, I., Pelissier, M.A. and Moser, T.J. [2013] Specularity Gathers for Diffraction Imaging, *75th EAGE Conference London, Extended Abstracts*.

Sturzu, I., Popovici, A.M., Pelissier, M.A., Wolak, J.M. and Moser, T.J. [2014] Diffraction imaging of the Eagle Ford shale, *First Break*, **32**, 49-59.